

Possible Light-Induced Superconductivity in a Strongly Correlated Electron System

Supplemental Material

Nikolaj Bittner,¹ Takami Tohyama,² Stefan Kaiser,^{1,3} and Dirk Manske¹

¹Max-Planck-Institut für Festkörperforschung, D-70569 Stuttgart, Germany

²Department of Applied Physics, Tokyo University of Science, Tokyo 125-8585, Japan

³4th Physics Institute, University of Stuttgart, D-70569 Stuttgart, Germany

A. INTERACTION QUENCH

Quench induced enhancement of the low energy peak in σ_1 . In Fig. S.1 we plot the temporal evolution of the magnitude of the low energy peak measured at frequency $\omega = 0$ in the real part of the optical conductivity spectrum ($\sigma_1(\Delta t, \omega = 0)$). Clearly, after quenching there is a sudden enhancement of $\sigma_1(\Delta t, \omega = 0)$ with the subsequent oscillations. At the same time, as discussed in the main text in connection to Fig.3, the CDW peak at $\omega \approx 1.8$ is completely disappeared. Thus, we can conclude that the spectral weight of the CDW peak is shifted into the low energy peak at $\omega = 0$.

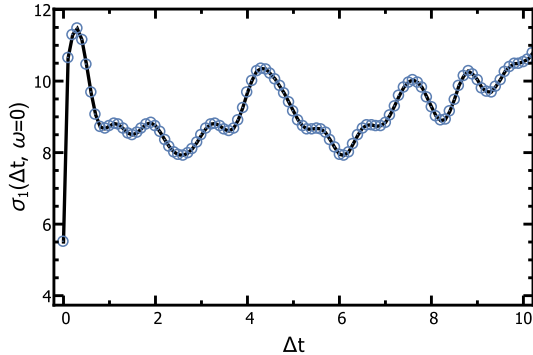


Figure S.1. (color online) Temporal evolution of the magnitude of the low energy peak ($\omega = 0$) in the $\sigma_1(\Delta t, \omega)$ spectrum after an interaction quench.

Quench induced enhancement in $\omega\Delta\sigma_2$. For characterization of the induced superfluid density we calculated $\langle\omega\Delta\sigma_2\rangle$ by fitting the $1/\omega$ divergence at low frequencies for each spectrum. We note that due to the finite size of our model we corrected σ_2 from the CDW contribution, i.e. $\Delta\sigma_2(\Delta t, \omega) = \sigma_2(\Delta t, \omega) - \sigma_2^{\text{eq, CDW}}$. The results are plotted in Fig. S.2 by the blue dashed line. As one can see from the figure, $\langle\omega\Delta\sigma_2\rangle$ shows a sudden enhancement after the quenching with the subsequent oscillations. This temporal behavior demonstrates dynamics reminiscent of

$\sigma_1(\Delta t, \omega = 0)$ (cf. Fig. S.1). Moreover, we compared the value of $\langle\omega\Delta\sigma_2\rangle$ with its equilibrium counterpart $\langle n \rangle_{\text{sc}}$ at $T = 0$ for the superconducting phase with $U = -4, V = -0.25$ and $\langle n \rangle_{\text{sc}} \sqrt{1 - T_{\text{eff}}/T_c}$, which are shown in Fig. S.2 by the blue and red solid lines, respectively. In the latter case we numerically estimated the ratio $T_{\text{eff}}/T_c = 0.8$. One can see that the temporal spectral weight of ω times σ_2 shows almost the same or even slightly larger values (at $\Delta t \approx 4, 7$ and 10) than in equilibrium, if the temperature due to the quench is taken into account (T_{eff}).

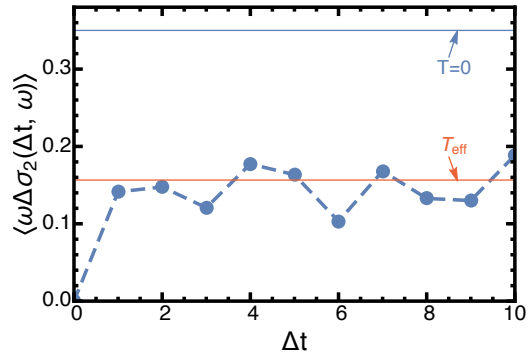


Figure S.2. (color online) Transient value of $\langle\omega\Delta\sigma_2(\Delta t, \omega)\rangle$ after an interaction quench (blue dashed line). The parameters of the quench are the same, as in the main text. The blue solid line corresponds to its equilibrium counterpart $\langle n \rangle_{\text{sc}}$ in the superconducting phase ($U = -4, V = -0.25$) at $T = 0$. The red solid line represents the value of $\langle\omega\Delta\sigma_2\rangle = \langle n \rangle_{\text{sc}} \sqrt{1 - T_{\text{eff}}/T_c}$ with the numerically estimated ratio $T_{\text{eff}}/T_c = 0.8$.

Cluster size dependence. Here, we compare the results of calculations for 10 and 14-sites lattice after identical quench excitation. We use the same quench protocol as described in the main text: the system is initially prepared in the CDW state with $U = -4$ and $V = 0.25$. At $t = 0$ the next-neighbour interaction strength is then suddenly changed by $\Delta V = -0.5$. The time-dependent results for density-density $C(j, t)$ and on-site $P_1(j, t)$ correlation functions are shown

in Fig. S.3. Clearly, for both 10 and 14-sites lattices $C(j, t)$ shows suppression of the characteristic for CDW "zigzag" structure after quenching. At the same time $P_1(j, t)$ illustrates strong enhancement of the superconducting correlations in nonequilibrium. This on-site correlation function in nonequilibrium shows a quite good agreement with the results for equilibrium superconducting state (dashed lines in Fig. S.3). All in all, for both 10 and 14-sites lattices we found similar behavior after quenching showing the enhancement of the superconducting correlations together with the suppression of the CDW structure.

B. PHASE QUENCH.

Characterization of eigenstates. For characterization of the initial phase with $U = -3$ and $V = 0.5$ in equilibrium, we plot in Figs. S.4 and S.5 on-site $P_1(j)$ and density-density $C(j)$ correlation functions for several low-energy eigenstates, respectively. Let us focus on the behavior of $C(j)$ (see Fig. S.5). Whereas in the ground state (blue dashed line) the density-density correlation function shows characteristic "zigzag" structure indicating alternating order of the electron density with mostly double occupied and empty sites, in the next two low-energy eigenstates (light red and red solid lines) it shows for $j > 2$ an almost constant behavior. On the other hand, the on-site correlation function shows no significant changes in the low-energy eigenstates (see Fig. S.4).

It should be noted that we adjust the central frequency of the pulse used for the phase quench (see

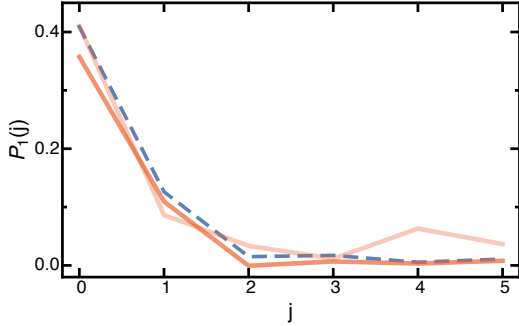


Figure S.4. (color online) On-site correlation function versus lattice distance j calculated for $U = -3$ and $V = 0.5$. The calculations are done exemplary for the first 3 eigenstates: ground state with $\Delta E=0$ (blue dashed line), $\Delta E_1 = 1.6295$ (light red solid line), and $\Delta E_2 = 2.5479$ (red solid line).

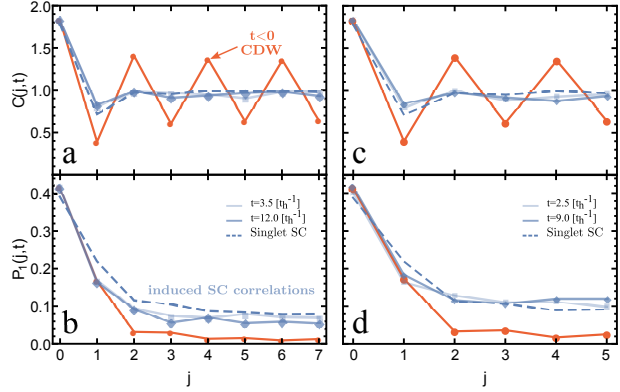


Figure S.3. (color online) Scaling dependence of (a), (c) the density-density and (b), (d) the on-site correlation functions obtained for the interaction quench ($U = -4$, $V = 0.25$, $\Delta V = -0.5$). Left panels correspond to the 14-site lattice, and right panels show results for the 10-site lattice. The color coding illustrates results at different times: red solid line corresponds to $t < 0$, light blue solid line represents $t = 3.5$ (14-site) and $t = 2.5$ (10-site), and blue solid line is for $t = 12$ (14-site) and $t = 9$ (10-site). Results for equilibrium SC phase are indicated by blue dashed lines.

main text) to the eigenstate, which is indicated in Figs. S.5 and S.4 by the red solid line.

Dynamical coexistence. Excitation spectrum and correlation function. To calculate an excitation spectrum we use the spectral representation of the stress tensor operator $\hat{\tau}$:

$$-\text{Im}\chi_{\tau\tau}(\omega) = \frac{1}{L} \sum_n |\langle n | \hat{\tau} | \text{GS} \rangle|^2 \delta(\omega - (\epsilon_n - \epsilon_0)/\hbar)$$

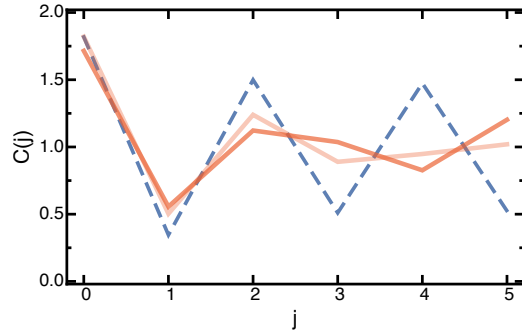


Figure S.5. (color online) Density-density correlation function versus lattice distance j calculated for $U = -3$ and $V = 0.5$. The calculations are done exemplary for the first 3 eigenstates: ground state with $\Delta E=0$ (blue dashed line), $\Delta E_1 = 1.6295$ (light red solid line), and $\Delta E_2 = 2.5479$ (red solid line).

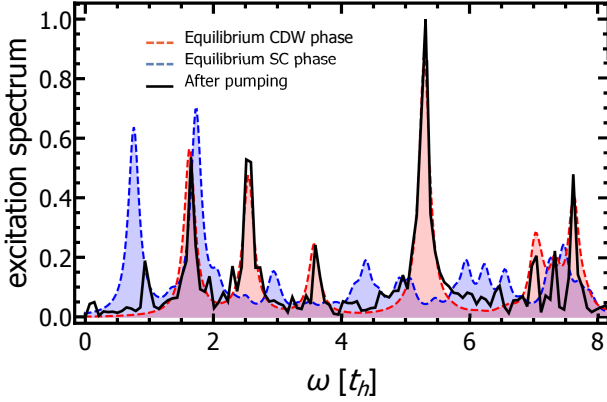


Figure S.6. (color online) Excitation spectrum of the system in nonequilibrium (black solid line) compared with the spectra in equilibrium singlet SC phase (blue region) and equilibrium CDW phase (red region).

where $\hat{\tau} = \sum_{j,\sigma} (t_h \hat{c}_{j+1,\sigma}^\dagger \hat{c}_{j,\sigma} + \text{H.c.})$ and $|n\rangle$ is the n -th eigenstate with the energy ϵ_n . For broadening of the spectral lines we use an artificial small number $\eta = 1/L$.

In Fig. S.6 we plot the excitation spectrum for initial CDW phase (red line) and equilibrium SC phase (blue line) together with the excitation spectrum after pumping (black line). Latter shows several distinct peaks. The most intensive peaks in the nonequilibrium spectrum can be identified with the initial equilibrium CDW phase. In fact, low energy peaks at $\omega \approx 1.5, 2.5$,

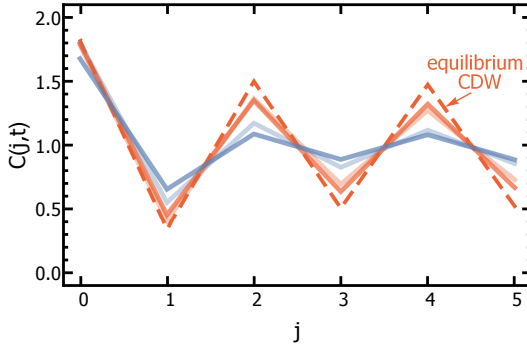


Figure S.7. (color online) Time-dependent density-density correlation function $C(j,t)$ as a function of the lattice site j obtained after a pump pulse excitation of the Gaussian shape. The parameters of the pulse are: $A_0 = 5$, $\omega = 2.38$, $\tau = 0.05$. The function $C(j,t)$ is exemplary shown at times: $t = 1$ (light red solid line), $t = 3$ (light blue solid line), $t = 5$ (red solid line), $t = 7$ (blue solid line). For comparison, the correlation function in equilibrium CDW phase is shown by the red dashed line.

3.5 and 5.5 match perfectly with excitation spectrum for the CDW phase. In addition, a peak at $\omega \approx 1.5$ might also represent an excited state of the singlet superconducting phase, since one of the most intensive peaks in the optical spectrum of the superconducting state appears at the same frequency. Additionally, a peak at $\omega \approx 1$ in the nonequilibrium spectrum can be assigned to the second intensive peak in the spectrum of the superconducting phase. Finally, some less intensive peaks at $\omega \approx 5$ and around $\omega \approx 6$ can be assigned to the superconducting phase.

To explore temporal evolution of the charged order, we plot in Fig. S.7 the time-dependent density-density correlation function $C(j,t)$. Before pumping the electron system is prepared in the equilibrium ground state of the CDW phase and $C(j,t)$ shows a characteristic "zigzag" structure (red dashed line). Clearly, the excitation of the system with the pulse leads to an effective partial suppression of the charge density wave correlations with the subsequent oscillations. It should be noted, that the system in nonequilibrium does not indicate any strong similarities with the first low-energy eigenstates of CDW (c.f. Fig. S.5).

Optical conductivity. Finally, in Fig. S.8 we show the time-dependent real part of the optical conduc-

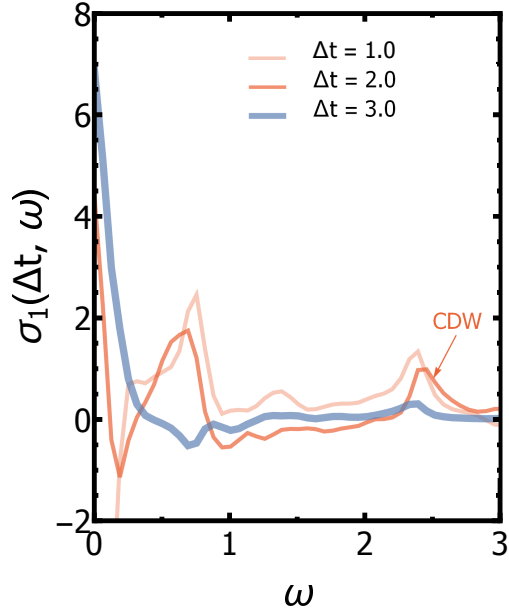


Figure S.8. (color online) (a) Time-dependent real conductivity $\sigma_1(\Delta t, \omega)$. Theoretically obtained results at different time delays are presented by the solid lines: $\Delta t=1$ (light red), $\Delta t=2$ (red), and $\Delta t=3$ (blue).

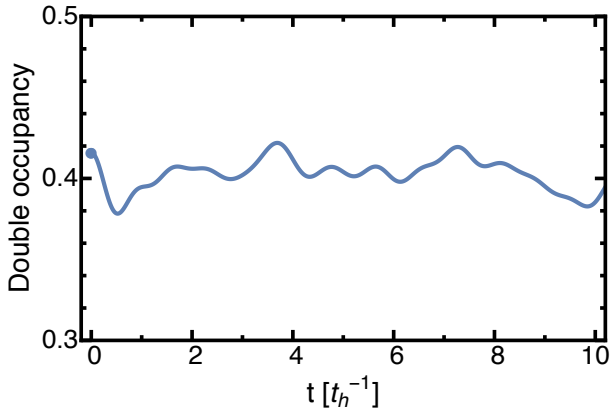


Figure S.9. (color online) Temporal evolution of the double occupancy function after the interaction quench. Blue dot indicates its value in equilibrium.

tivity $\sigma_1(\Delta t, \omega)$. In agreement with the results for the imaginary conductivity $\sigma_2(\Delta t, \omega)$ [see Fig. 5 in the main text] we observe first a partial reduction of the spectral weight of the low energy peak corresponding to the equilibrium CDW state at both $\Delta t = 1$ (light red solid line) and $\Delta t = 2$ (red solid line) with the appearance of an in-gap state at $\omega \approx 0.7$. At $\Delta t = 3$ the response from CDW is disappeared and the spectral weight is shifted to a low-energy peak at $\omega \approx 0$ representing a transient δ -peak.

C. DOUBLE OCCUPANCY FUNCTION

In order to get an additional insight into the charge dynamics after the interaction and the phase quench we plot in Figs. S.9 and S.10 time-dependent double occupation function. After the interaction quench double occupation function shows oscillations with a quite small magnitude (see Fig. S.9). Physically this behavior can be interpreted as a redistribution of the electron pairs on the lattice initially prepared in the CDW phase, which was initiated by the interaction quench.

In case of the pulse quench (see Fig. S.10) we find in the behavior of the double occupancy function an effective decrease with strong oscillations around a new reduced value. Physically, it means that the excitation of the electron system leads to a dynamical breaking and creation of the electron pairs on a lattice. Moreover, at some moments in time (e.g. at $t \approx 3$ etc.) one can observe a recovery of the double occupation function to its initial value. Since the charge density wave correlations are partially suppressed after pump-

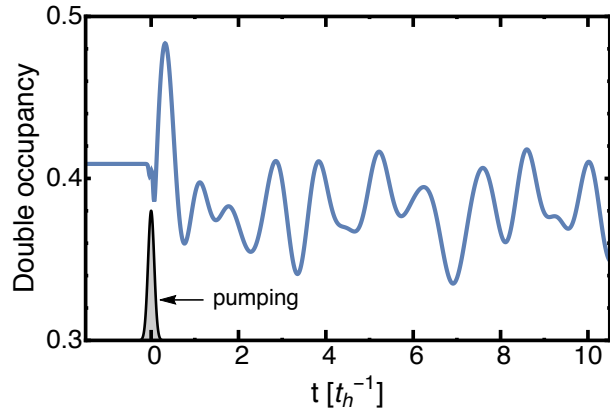


Figure S.10. (color online) Temporal evolution of the double occupancy function after the phase quench.

ing (see Fig. S.7), this behavior indicates a transient redistribution of the electron pairs on the lattice.